ELSEVIER

Colloids and Surfaces
A: Physicochemical and Engineering Aspects 209 (2002) 83–104

COLLOIDS AND SURFACES A

www.elsevier.com/locate/colsurfa

Capillary mechanisms in membrane emulsification: oil-in-water emulsions stabilized by Tween 20 and milk proteins

N.C. Christov, D.N. Ganchev, N.D. Vassileva, N.D. Denkov, K.D. Danov, P.A. Kralchevsky *

Laboratory of Chemical Physics & Engineering, Faculty of Chemistry, University of Sofia, 1 James Bourchier Ave., Sofia 1164, Bulgaria

Received 10 December 2001; accepted 22 March 2002

Abstract

We investigate the process of membrane emulsification in the presence of the nonionic surfactant Tween 20, and the milk proteins Na-caseinate and beta-lactoglobulin (BLG). Our goal is to examine the factors which control the drop-size distribution in the formed emulsions. The drops are produced at the outer surface of a cylindrical microporous glass membrane, so that the process of their formation and detachment can be directly observed by an optical microscope. In the case of 2 wt.% aqueous solution of Tween 20 we obtain a relatively fine and monodisperse oil-in-water emulsion with a mean drop diameter about three times that of the pore. The microscopic observations show that in this case the oil drops intensively pop out of separate pores. In contrast, for the lower concentrations of Tween 20, as well as for the investigated solutions of Na-caseinate and BLG, we observe that the membrane is covered by a layer of growing attached emulsion drops, which are polydisperse, with a relatively large mean drop size. This fact can be explained with a greater dynamic contact angle solid-water-oil. In such a case, after a drop protrudes from an opening, it does not immediately detach, but instead, the contact area drop/membrane expands over several pore openings. The smaller drop size in the emulsions stabilized by BLG, in comparison with those stabilized by Na-caseinate, is related to the circumstance that BLG adsorbs faster at the oil-water interface than Na-caseinate. In the investigated emulsions we did not observe any pronounced coalescence of oil drops. Hence, the generation of larger and polydisperse oil drops in some of the studied solutions is attributed mostly to the effect of expansion of the drop contact line and formation of hydrophobized domains on the membrane surface. Therefore, any factor, which leads to decrease of the dynamic three-phase contact angle, and thus prevents the contact-line expansion, facilitates the production of fine and monodisperse emulsions.

Keywords: Membrane emulsification; Oil-in-water emulsions; Dynamic interfacial tension; Milk proteins; Kinetic barrier to adsorption

* Corresponding author. Tel.: +359-2-962-5310; fax: +359-2-962-5643.
E-mail address: pk@lcpe.uni-sofia.bg (P.A. Kralchevsky).

0927-7757/02/$ - see front matter
PII: S0927-7757(02)00167-X

1. Introduction

1.1. Studies on membrane emulsification

The method of membrane emulsification, proposed by Nakashima et al. [1,2], has found a considerable development and many applications during the last decade [3–39]. The influence of different factors on the process of emulsification by microporous membranes has been investigated in the works by Kandori et al. [3,4,6], Asano et al. [8,9,17,33,34], Schubert and Schröder [19–21], Williams et al. [22–24], and Yuyama et al. [37–39]. The method has been applied in many fields, in which monodisperse emulsions are needed. An example is the application in food industry for production of oil-in-water (O/W) emulsions: dressings, artificial milk, cream liqueurs, as well as for preparation of some water-in-oil (W/O) emulsions: margarine and low-fat spreads [5–10,17,32–35]. Another application of this method is for fabrication of monodisperse colloidal particles: silica-hydrogel and polymer microspheres; porous and cross-linked polymer particles; microspheres containing carbon black for toners, etc. [4,11,12,18,25–31,38,39]. A third field of utilization is for obtaining multiple emulsions and micro-capsules, which have found applications in pharmacy and chemotherapy [13–16]. A recent review can be found in [36]. Closely related to the membrane emulsification is the method employing capillary tubes and micro-channels to produce monodisperse emulsions [40–45]. Studies on the detachment of emulsion drops from the tip of a single capillary have been also carried out [46–48].

1.2. Factors affecting the emulsion drop size

A key problem of membrane emulsification is to explain and predict the dependence of the mean drop diameter, d_{drop}, on the experimental parameters: mean pore diameter, d_{pore}, applied cross flow in the continuous phase, flux of the disperse phase along the pores, viscosity of the oil and water phases, interfacial tension and kinetics of surfactant adsorption, etc. (Here and hereafter we call 'disperse' the phase from which the drops are made, despite the fact that this phase is continuous before the drop detachment from the membrane.) The values of the ratio d_{drop}/d_{pore}, reported in different experimental works, vary in the range from 2 to 10 [36]; the reasons for this variation have not yet been well understood. Below we briefly consider the major factors affecting the ratio d_{drop}/d_{pore}.

The experiment shows that the presence of crossflow (stirring) in the continuous phase decreases the size of the oil drops, which are detaching from the emulsification membrane [20,21,23,32,35,36,47]. This fact can be explained with the action of a hydrodynamic drag force, which helps the emulsion drops to brake away [23,47,49]. Ito et al. [47] have obtained a semiempirical theoretical expression, which agrees very well with the experimental dependence of the drop volume on the applied shear rate (characterized by the Weber number) in the case, when there is no surfactant dissolved in either of the two liquid phases. The approach by Ito et al. [47] uses the diameter of the drops, formed in the absence of crossflow, as an input parameter. In the latter case (no cross flow), the experiment shows that $d_{drop}/d_{pore} > 3 \pm 0.5$. On the other hand, values $d_{drop}/d_{pore} < 3$ are typical for experiments, which are carried out in the presence of sufficiently intensive crossflow, supposedly the disperse phase does not wet the membrane [2]. (If the disperse phase wets the membrane, one obtains emulsions with $d_{drop}/d_{pore} > 3.5$ even in the presence of considerable stirring; this issue is discussed in details in Section 6 below.)

The flux of the disperse phase along the pores of the emulsification membrane can be varied by controlling the pressure difference applied across the membrane. The experiments show that typically an increase of the transmembrane flow (or of the applied pressure) results in a greater mean drop size and in a higher polydispersity of the formed drops [9,19,21,32,37]. Moreover, one can distinguish two regimes of transmembrane flow: (i) fixed flow rate and (ii) fixed pressure. The former regime takes place in the emulsification setups using a bunch of capillaries or micro-channels, where the disperse phase is usually supplied by a pump [40–45]. The second regime is typical

for the standard emulsification setups, in which the disperse phase is pushed across the membrane by nitrogen gas from a bottle [2,5,9,14,20]. In this case the gas plays the role of a buffer which keeps constant the applied pressure difference across the membrane; on the other hand, the flow rate along a given pore may oscillate when drops grow and detach at its orifice.

The oil–water interfacial tension, σ, is recognized to be the major retention force, that is the force which keeps the drops attached to the membrane surface [19,21,46]. Greater σ is expected to cause the production of larger emulsion drops. Complications arise from the fact that, as a rule, a surfactant (emulsifier) is dissolved in the continuous phase to stabilize the produced emulsion against drop coalescence. Since the surfactant has a finite rate of adsorption at the oil–water interface [50], the coverage of the drop surface with adsorbed surfactant molecules decreases (and the dynamic value of σ increases) when the frequency of drop release from the pores grows. The latter effect could explain, at least in part, the aforementioned rise in the drop size with the increase of the transmembrane pressure.

Another factor, related to the surfactant adsorption, is the role of coalescence for establishment of the drop-size distribution. The low coverage of the drop surfaces with adsorbed surfactant leads (i) to a larger interfacial tension and (ii) to a drop coalescence in the formed emulsion. The latter two effects have the same consequence: appearance of larger drops. It should be clarified which effect [(i) or (ii), or both] is more important for the observed formation of larger drops (of diameter greater than three times the pore diameter). It is possible to have coalescence of emulsion drops at the membrane surface (during their formation) and later, in the bulk of the formed emulsion [19]. To our surprise, it turns out that neither of the aforementioned effects is decisive for the appearance of larger drops ($d_{drop}/d_{pore} > 4$) in the emulsions studied by us (in Section 6 we describe the actual mechanism of large drop formation, which involves an expansion of the contact area drop/membrane over several pore openings).

Last, but not least, the membrane hydrophilicity/hydrophobicity also influences the drop size and monodispersity. In the first experiments by Nakashima et al. [2] it became clear that the membrane should be initially soaked and wet by the continuous phase for fine and monodisperse emulsion to be produced. The effect of membrane wettability was noticed by several authors [2,8,17,37]; some of them characterized the used membranes with the respective solid–water–oil contact angle. It has been established experimentally that more hydrophilic membranes produce finer O/W emulsions with a better monodispersity, and vice versa [2,37].

1.3. Aim and structure of the paper

Our paper is aimed at investigating the relative importance of several factors for the occurrence of the membrane emulsification with O/W food emulsions. With such emulsions, the greatest differences between the size distributions of the produced drops have been registered, depending on the emulsifier type and concentration [8,17,32,34,36]. In contrast with the preceding studies, in which the emulsion drops have been formed at the inner surface of a tubular membrane, we employ a special setup for producing the drops at the outer membrane surface (Fig. 1). In the former regime of emulsification, the membrane could sustain larger applied transmembrane pressures, but one cannot observe the actual pro-

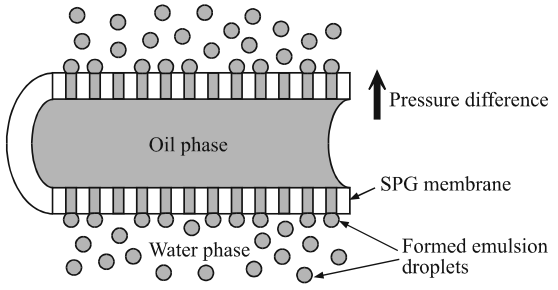

Fig. 1. Sketch of the used membrane emulsification method: the oil phase is supplied under pressure in a tubular microporous glass membrane; the emulsion drops appear at the outer surface of the membrane, which is immersed in the water phase.

cess of drop formation at the microporous surface, which is hidden inside the non-transparent tube. In contrast, the setup sketched in Fig. 1 enables one to observe directly the processes at the membrane surface and to relate the distribution of the produced emulsion drops with the elementary acts of drop formation and detachment.

In this paper we focus our attention (i) at the role of the surfactant adsorption and dynamic interfacial tension and (ii) at the effect of membrane hydrophilicity on the drop size distribution. For that reason, in the present study we do not apply a cross flow in the continuous phase (such flow would also influence the drop size). As mentioned above, the approach by Ito et al. [47], allows one to determine the mean drop diameter for a given crossflow rate, if the drop diameter in the absence of stirring is known. In this way, the problem is reduced to determining the mean drop diameter, and the factors influencing it, in the absence of crossflow (stirring). The latter problem is the subject of the present study.

The paper is organized as follows. In the next section we describe the used methods and materials. In Section 3 we report results for production of O/W emulsions by microporous membranes using Tween 20 as emulsifier; we present and interrelate experimental drop-size distributions and photographs of drop formation at the membrane surface. Section 4 and Section 5 contain similar data, but for the milk proteins Na-caseinate and β-lactoglobulin (BLG). Finally, in Section 6, we discuss and interpret the experimental results for the process of membrane emulsification in an attempt to identify the underlying capillary mechanisms.

2. Methods and materials

2.1. Membrane emulsification apparatus and procedure

In our experiments we used a Microkit membrane emulsification module (SPG Technology, Miyazaki, Japan), which works with tubular type Shirasu porous glass membranes of outer diameter 10 mm, thickness 1 mm and working area of approximately 3 cm^2. Membranes of different average pore diameter are available: from 1 to 20 μm. According to the manufacturer, the porosity (the surface fraction of the pores) is about 50%. The working pressure difference is up to 10^5 Pa. As the membranes are made of hydrophilic glass, they are suitable for producing O/W emulsions, which is the type of emulsions investigated by us. (After hydrophobization, the membranes can be used also for generating W/O emulsions.) All experiments were carried out at temperature $T = 23 \pm 2$ °C.

As mentioned above, one of our aims is to observe the emulsion drops in the moment of their detachment from the membrane. Therefore, to produce O/W emulsions, the oil phase is supplied inside the tubular membrane, and the oil drops are released in the outer aqueous phase (Fig. 1); this is the so called 'batch method' [6]. The higher pressure in the oil is provided by a gas (N_2) bottle. We do not apply a cross flow in the outer aqueous phase. The only directed motion of the formed oil droplets occurs under the action of the buoyancy force. The membrane and the water phase are placed in a cuvette from optical glass (Hellma GmbH, Müllheim, Germany), which enables one to directly observe the emulsification process at the membrane surface. For that purpose, we used a CCD camera with an attached long-focus objective: CTL-6 (Tokyo Electronic Industry Co., Japan) with magnification × 6 and working distance 39 mm.

After the end of every emulsification experiment, the used membrane has been recovered by means of the following procedure: (i) soaking in 2 wt.% solution of AOT in ethanol for 2 h; (ii) rinsing and soaking in pure water; (iii) immersion for 1 h in water solution of 2 M HCl at 70 °C; (iv) rinsing and soaking in pure water for 30 min. Our practice shows that this procedure fully recovers the initial hydrophilic state of the SPG membranes, which can be used in subsequent experiments.

In the beginning of each experiment, the tubular membrane is first fixed at the holder of the emulsification setup and immersed in the aqueous surfactant solution. Then, the oily phase is sup-

plied under pressure. We start with an initial pressure that is not sufficiently high for the oil to displace the aqueous phase from the pores of the membrane, and consequently, emulsification is not observed. Next, the pressure is gradually increased, until the emulsification begins at a certain threshold (critical) pressure, P_{cr} [2]. The working pressure, P, during the emulsification experiment is afterwards fixed at a value, which is slightly (with less than 10%) greater than P_{cr}.

The critical pressure can be estimated from the equation $P_{cr} = (4\sigma_{ow} \cos \alpha)/d_{pore}$, where σ_{ow} is the oil–water interfacial tension and α is the membrane–water–oil contact angle (measured across water) [2]. Since σ_{ow} and α depend on the bulk surfactant concentration, the interfacial age (frequency of drop release), and the pore diameter, in our experiments P_{cr}, as well as the flux of oil across the membrane, was different for the different used solutions and membranes. As already mentioned, the fixed parameter in our experiments was $P/P_{cr} \approx 1$.

In other experiments, we varied the transmembrane pressure, P, in a certain range above P_{cr}. The formed emulsions were markedly more polydisperse, in agreement with the results of other authors [9,19,21,32,37], and in consonance with the hydrodynamic theory of drop detachment [51].

2.2. Determination of the drop size distribution

Representative samples of the produced emulsions were observed in transmitted light by microscope Nikon Optiphot 2 with objectives $\times 100$ and $\times 50$. The specimens were prepared by placing a small portion of the emulsion in a cytometric glass cell. The resolution of the used optical microscope is 0.8–1 μm; consequently, this is the lower limit for precise measurements of drop diameters in our experiments. The microscopic pictures were recorded by means of a high resolution CCD camera (Sony) and digital memory VCR (Panasonic WV-5490). The images were processed using a semi-automatic image analysis software, operating with Targa + graphic board (True Vision, USA). To determine the size distribution in a given emulsion, the diameters of several hundred droplets (at least 300) were measured and recorded. To decrease the probability for systematic errors, the measurements were performed with, at least, six different randomly chosen frames. All droplets on the frames were taken into account, even the smallest ones which were still visible. The collected data were used to obtain the drop size distribution in the form of histograms or line-and-scatter plots (see below).

2.3. Materials

As oil phase in our experiments we used hexadecane ($C_{16}H_{34}$), product of Sigma (without additional purification), and soybean oil. The latter was purified by passing through a glass column filled with the chromatographic adsorbent Florisil.

In some experiments, as aqueous phase we used solutions of the nonionic surfactant Tween 20 (polyoxyethylene-20 sorbitan monolaurate), product of Merck. No electrolyte was added. In other experiments, we used water solutions of proteins, such as β-lactoglobulin (BLG) and sodium caseinate (both of them products of Sigma), as well as mixed solutions of BLG and Tween 20. All protein solutions contained also 0.1 g l^{-1} NaN_3 for antibacterial protection.

3. Results for solutions of Tween 20

3.1. Emulsions in 2 wt.% solutions of Tween 20

Fig. 2 shows the size distribution of hexadecane drops formed by membrane emulsification (pore diameters $d_{pore} = 1.0$ and 3.2 μm) in a 2 wt.% aqueous solution of Tween 20. The distribution in Fig. 2(a) has two peaks, the major one being at drop diameter $d_1 = 3.0 \pm 0.2$ μm. The distribution in Fig. 2(b) has a well pronounced single peak at $d_{drop} = 9.8 \pm 0.1$ μm, that is at $d_{drop}/d_{pore} \approx 3.06$. The same value of the ratio $d_{drop}/d_{pore} \approx 3$ has been reported in other membrane-emulsification experiments [2,5,6,14,19,35,36]. The hydrodynamic theory of drop detachment [51] really predicts $d_{drop}/d_{pore} \approx 3$ for transmembrane pressure equal to the critical one (for commencement of

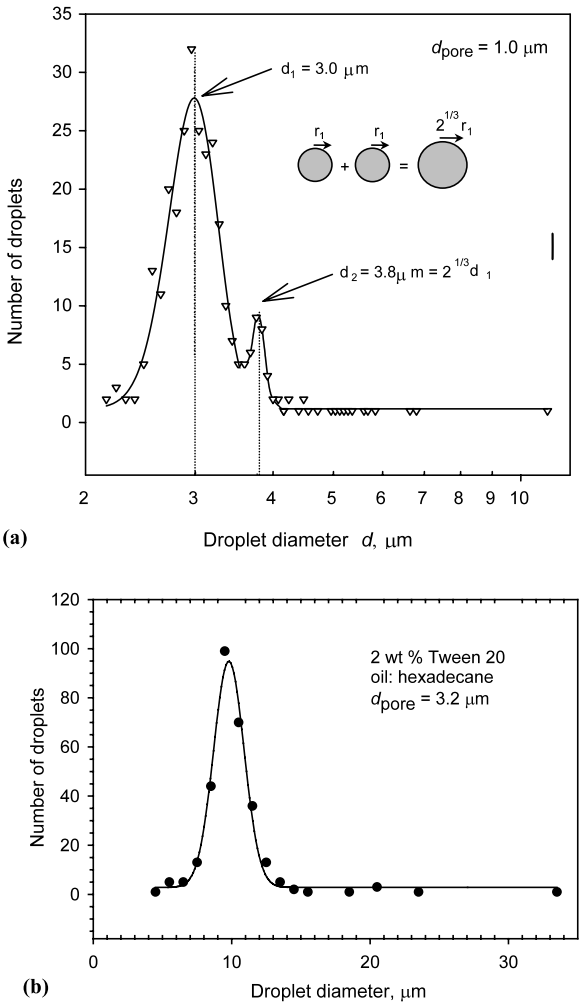

Fig. 2. Size distribution of hexadecane drops formed by membrane emulsification in 2 wt.% water solution of Tween 20; the water and oil phases are pre-equilibrated; diameters of 300 drops are measured: (a) pore diameter 1.0 μm; (b) pore diameter 3.2 μm; the curve is a Gaussian fit, see Eq. (1).

emulsification) and in the absence of cross flow in the continuous phase.

The secondary peak in Fig. 2(a), which appears at $d_2 \approx 3.8$ μm, can be explained as a result of drop coalescence. Indeed, if two drops of volume V_1 coalesce, the resulting bigger drop will have volume $V_2 = 2V_1$, which implies $d_2 = 2^{1/3}d_1$. With $d_1 = 3$ μm, this really yields $d_2 \approx 3.8$ μm, as experimentally observed. The fact that the secondary peak is much smaller than the major one (Fig. 2(a)), indicates the presence of a weak drop coalescence. Most probably, the drops have coalesced in the produced emulsion: due to the buoyancy force the drops emerge to form a cream in the upper part of the cuvette. There, the drops rest in a close contact with each other and some of them could coalesce. The absence of a secondary peak in Fig. 2(b) can be explained with the fact that the sample for drop-size measurement has been taken immediately after the production of the emulsion. In particular, Fig. 2(b) demonstrates that it is possible to obtain emulsions with $d_{drop}/d_{pore} \approx 3$ and with a narrow drop-size distribution under unstirred conditions. Our experiments indicate that such results can be obtained if the following two necessary conditions are satisfied: (i) The transmembrane pressure is equal, or slightly (with less than 10%) greater, than the critical (threshold) pressure for drop production, and (ii) the continuous (aqueous) phase wets well the membrane. In addition, if stirring is applied, one can achieve $d_{drop}/d_{pore} < 3$, see e.g. [47].

3.2. Effect of pre-equilibration of oil versus water phases

It is worthwhile noting that Tween 20 is soluble not only in the aqueous, but also in the oily phase. The data in Fig. 2 are obtained with hexadecane, which was pre-equilibrated with the surfactant solution. If the two phases are not equilibrated, one may expect a lower surfactant adsorption at the oil–water interface, which implies higher interfacial tension and easier coalescence of the emulsion drops upon collision [52]. Moreover, some dynamic phenomena, like the cyclic dimpling [53] and osmotic swelling [54], have been observed with emulsion films from non-equilibrated phases. To check whether the pre-equilibration of the oil and water phases is important for the membrane emulsification, in Fig. 3 we compare the drop-size distributions obtained with pre-equilibrated and non-equilibrated phases. (The distribution for pre-equilibrated phases is the same as in Fig. 2(a)). One sees that the fraction of the larger drops is slightly greater in the case of non-equilibrated emulsions. For statistical analysis of the drop-size distribu-

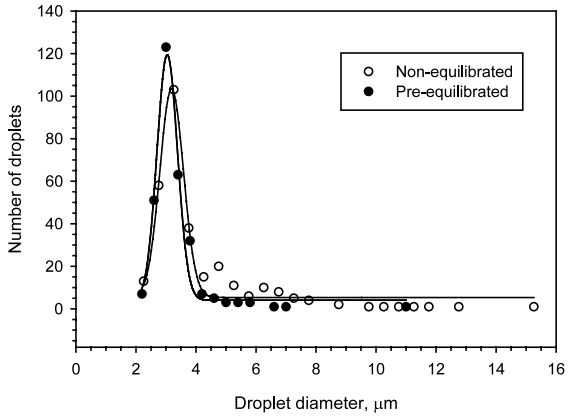

Fig. 3. Comparison of the size distributions obtained by membrane emulsification (pore diameter 1 μm) using pre-equilibrated and non-equilibrated hexadecane and water phases; 2 wt.% Tween 20 were initially dissolved in the water phase; for each distribution diameters of 300 drops are measured; the curves are Gaussian fits, see Table 1.

tion, we fitted the data points with a 4-parameter Gaussian curve:

$$N(d) = N_0 + a \exp\left[-\frac{(d - d_m)^2}{2b^2} \right] \quad (1)$$

where N denotes the number of drops; d is the drop diameter, d_m is its most probable value, corresponding to the maximum of the Gaussian curve (Fig. 3), b is the half-width of the peak, N_0 characterizes the background at which the peak appears, and a is a scaling parameter. We determined the parameters of the best fit using a commercially available software (Sigma Plot 6.0, SPSS Inc.) The parameters, corresponding to the two curves in Fig. 3, are listed in Table 1. The multiple correlation coefficient, R, is a measure of how well the regression curve describes the data ($0 \leq R \leq 1$). R values near 1 indicate that the model curve agrees well with the experimental points.

The values of R in Table 1 show that the size distributions in both types of emulsions are fitted well by a Gaussian curve. The Gaussian character of the distribution is, most probably, due to the random, essentially non-equilibrium, character of the drop detachment (by a necking instability), and to the non-uniformity in the pore sizes. The values of d_m, b and N_0 are slightly greater for the case of non-equilibrated phases. We could attribute the difference between the two size-distributions to the effect of a weak coalescence in the emulsion produced from non-equilibrated phases, or to the effect of contact-line expansion, which is discussed in Section 6 below. The obtained small differences (Table 1) indicate that the effect of pre-equilibration turns out to be insignificant, at least for the investigated system. In contrast, as demonstrated in the next section, the variation of surfactant concentration may have a dramatic effect.

3.3. Effect of the concentration of Tween 20

Fig. 4 shows experimental size distributions of hexadecane drops formed by membrane emulsification (pore size 1.0 μm) for three concentrations, 0.02, 0.2 and 2 wt.% Tween 20. For Tween 20 we have $\mathrm{CMC} \approx 2.8 \times 10^{-5}$ M, that is the above three working concentrations correspond to ≈ 6, 60 and 600 times the CMC, respectively. The oil and water phases have been pre-equilibrated. For each concentration, the diameters of 300 drops have been measured.

It is seen in Fig. 4 that the peak at $d_{drop} \approx 3$ μm is predominant for 2 wt.%, whereas at the lower concentrations, 0.02 and 0.2 wt.%, the fraction of the larger drops prevails, although the peak at 3 μm is still present. To find the reasons for the differences between the obtained drop-size distri-

Table 1
Parameters of the Gaussian fits in Fig. 3 drawn by means of Eq. (1)

State of the oil and water phases	d_m (μm)	b (μm)	N_0	R
Non-equilibrated	3.19 ± 0.03	0.39 ± 0.03	5.3 ± 1.4	0.98
Pre-equilibrated	3.04 ± 0.02	0.34 ± 0.03	4.1 ± 2.4	0.99

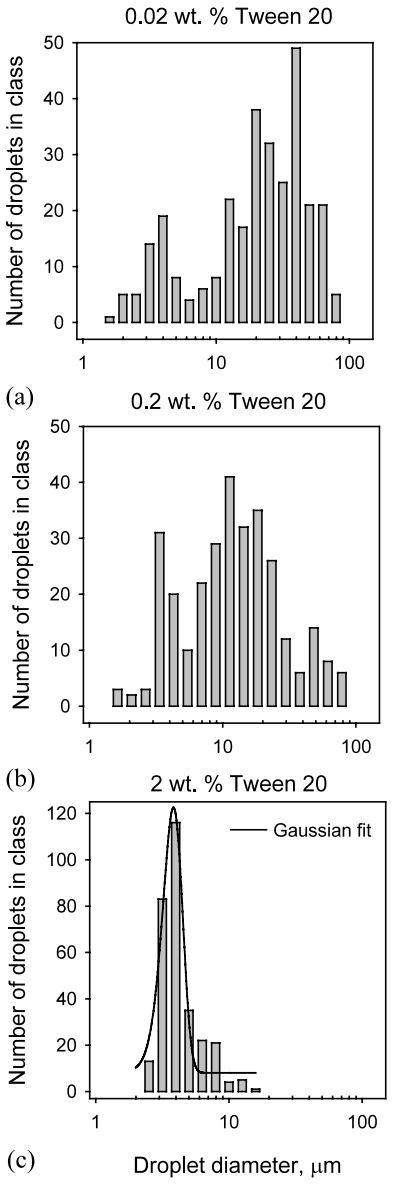

Fig. 4. Comparison of size distributions of hexadecane drops formed by membrane emulsification (pore diameter 1 μm) for three concentrations (a) 0.02 wt.%, (b) 0.2 wt.% and (c) 2 wt.% Tween 20; for each distribution diameters of 300 drops are measured.

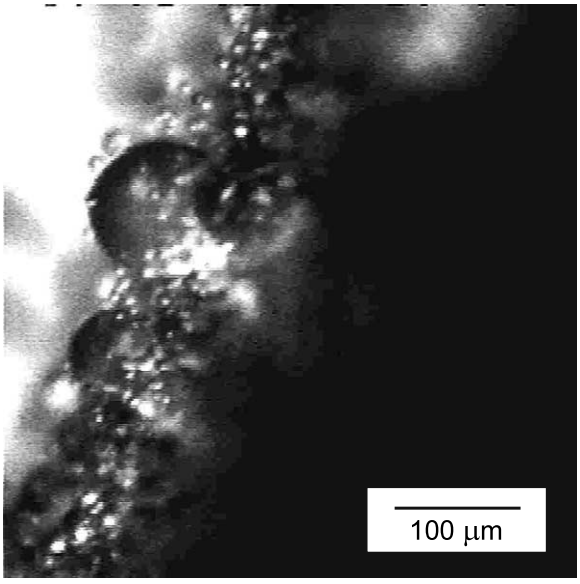

(a)

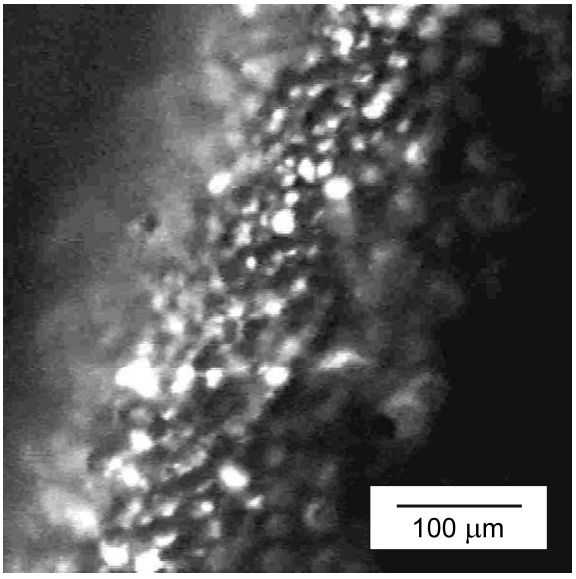

(b)

Fig. 5. Photos of the outer surface of a microporous glass membrane taken during the process of emulsification; the drops are of hexadecane in water solutions: (a) 0.02 wt.% Tween 20, pore size 3.2 μm; (b) 2 wt.% Tween 20, pore size 10.4 μm.

butions, we carried out direct observations of the drops, at the moment of their formation and release from the membrane surface.

Typical video-frames of the membrane surface, taken during the process of emulsification of hexadecane in solutions of Tween 20 at concentra-

tions 0.02 and 2 wt.% are shown in Fig. 5(a) and (b), respectively. To produce drops of greater size, which are better visible by optical microscope, we used membranes with larger pores, viz. $d_{pore} = 3.2$ and 10.4 μm.

At concentration 0.02 wt.% Tween 20, we observed simultaneous formation of small oil drops ($d_{drop}/d_{pore} \approx 3$) and larger oil drops ($d_{drop}/d_{pore} \gg 3$) at the membrane surface (Fig. 5(a)), which is in agreement with the size distribution shown in Fig. 4(a). The small drops are quickly emitted from membrane pores; the dynamics of their detachment resembles the release of gas bubbles in the maximum bubble pressure method [55,56]. In contrast, the larger drops are observed to stay and grow attached to the membrane surface for relatively longer periods of time, from several seconds to dozens of seconds. A closer examination of the video-records shows that a larger drop originates from a small drop, whose ejection from the pore is accompanied by expansion of its three-phase contact line. Thus a larger drop is formed attached to the membrane. In fact, the whole membrane surface is covered with a layer of larger drops, which stay attached, gradually increase in size, and eventually detach. The smaller drops are emitted from pores situated in-between the larger drops.

At concentration 2 wt.% only small drops ($d_{drop}/d_{pore} \approx 3$) are formed, which are swiftly ejected from the pores (Fig. 5(b)). This observation is consonant with the size distribution in Fig. 3 and Fig. 4(c). We occasionally observed detachment of larger drops from few isolated small domains on the membrane surface, but such larger drops seem to be an exclusion, which contribute to the background of the drop-size distribution (see Fig. 3 and Table 1). The domains of question are most probably hydrophobized spots on the membrane surface, see Section 6 for a more detailed discussion.

We examined carefully the video-records to identify acts of coalescence of oil drops at the membrane surface. For the lower concentration, 0.02 wt.% Tween 20, we observed only a few acts of coalescence; for the higher concentration, 2 wt.% Tween 20, we could not observe any. (As already mentioned, the secondary peak in Fig. 2(a) can be attributed to a weak coalescence in the produced emulsion cream.) In general, the coalescence of emulsion drops in these experiments is a very rare phenomenon. On the other hand, as explained above, the formation of larger drops ($d_{drop}/d_{pore} > 3$), which is typical for 0.02 wt.% Tween 20 (Fig. 5(a)), occurs through expansion of the contact line of forming attached drops; see Section 6 for further explanations.

4. Membrane emulsification with milk proteins

4.1. Experiments with Na-caseinate

We applied membrane emulsification (pore size 1.0 μm) to form emulsions from hexadecane in aqueous solutions of Na-caseinate without added electrolyte. At Na-caseinate concentration 0.01 wt.%, it was impossible to produce emulsion; instead, we observed the formation of a cream of millimeter-sized drops adhering to the membrane. In 3–4 min, the drops in this adherent cream coalesced and formed an oil layer covering the membrane. This is the only case with pronounced coalescence observed in our experiments.

At ten times larger concentration, 0.1 wt.% Na-caseinate, it was possible to produce emulsion, which contained large drops with a relatively broad size-distribution: the drop diameters ranged from 3 to 300 μm. At higher concentrations, 1 and 3 wt.% Na-caseinate, the produced emulsions had slightly smaller drops and narrower size distributions, see Fig. 6. The respective mean drop diameters, $d_{drop} \approx 33$ and 31 μm, are close to each other, see Table 2. The half-widths of the respective Gaussian fits are relatively large, $b \approx 7$ and 11 μm. Despite some scattering of the data, reflected by the higher values of N_0 (cf. Table 1), the size distributions are fitted well by Gaussian curves, which is evidenced by the value $R = 0.97$ in Table 2.

The above results rise the question why the ratio d_{drop}/d_{pore} is about 10 times greater for Na-caseinate in comparison with 2 wt % Tween 20 (cf. Figs. 3 and 6). To get some additional information, we carried out direct microscopic observations of the membrane emulsification process

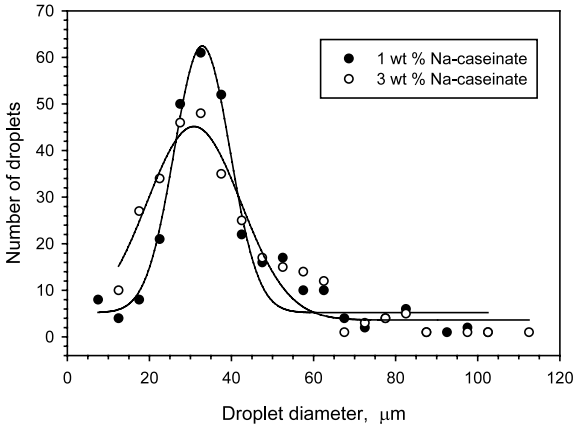

Fig. 6. Size distributions of hexadecane drops formed by membrane emulsification (pore diameter 1 μm) in water solutions containing 1 and 3 wt.% Na-Caseinate; for each distribution diameters of 300 drops are measured; the curves are Gaussian fits, see Table 2.

for solutions containing Na-caseinate, see Fig. 7(a). We observed the formation of a layer of relatively large oil drops adherent to the membrane surface. The major difference with Fig. 5(a) is that the small drops ($d_{drop}/d_{pore} \approx 3$) are missing. The adherent layer of oil drops (Fig. 7(a)) is dynamic: the drops grow, detach and new drops are formed on their place. At concentrations 1 and 3 wt.% Na-caseinate, we did not observe any pronounced coalescence of oil drops in the adherent layer. The results of these experiments are discussed and interpreted in Section 6.

4.2. β-Lactoglobulin in comparison with Na-caseinate

At concentration 1 wt.% β-lactoglobulin (BLG) we also observed the presence of transiently adherent oil drops at the membrane surface (Fig. 7(b)). The main difference in comparison with Na-caseinate is that for BLG the average drop size is considerably smaller. This can be seen also in Fig. 8, where the drop size distributions in emulsions, formed by membrane emulsification ($d_{pore} = 1.0$ and 2.1 μm) in solutions containing 1 wt.% BLG and 1 wt.% Na-Caseinate, are compared. One sees that in the case of BLG the most probable diameter and the half-width of the Gaussian curve (Table 3) are several times smaller in comparison with those for Na-caseinate. In particular, for $d_{pore} = 1.0$ μm we obtain $d_m \approx 6$ versus 33 μm and $b \approx 1$ versus 6 μm. The situation is similar for the membrane with $d_{pore} = 2.1$ μm (Fig. 8(b) and Table 3). The drop size distributions for both BLG and Na-caseinate are fitted well by Gaussian curves.

We conducted comparative experiments on emulsification by a common rotor-stator homogenizer Ultra Turrax T25 (Janke & Kunkel GmbH & Co.). Emulsions containing 30 vol.% of oil were prepared by stirring the oil–protein solution mixture for 3 min at 20 500 rpm. The results for 1 wt.% BLG solutions are compared in Fig. 9 and Table 3 with those for emulsions produced by membrane emulsification, pore size 1 μm. One sees that in this specific case, the emulsion produced by Ultra Turrax has smaller mean drop size. The relative width of the Gaussian peak is comparable: $b/d_m = 0.25$ and 0.26 for membrane of 1 μm pores and Ultra Turrax. On the other hand, the background, N_0, is higher in the case of Ultra-Turrax, in comparison with the membrane emulsification (Table 3). The microscopic observations showed that the membrane-produced emulsion does not contain drops of diameters smaller than d_{pore}, whereas the emulsion obtained by Ultra Turrax contains even sub-μm drops; in the latter case the Gaussian peak appears on the background of drops of various size.

Table 2
Parameters of the Gaussian fits in Fig. 6 drawn by means of Eq. (1)

Concentration of Na-Caseinate	d_m (μm)	b (μm)	N_0	R
1 wt.%	32.9 ± 0.5	6.8 ± 0.5	5.2 ± 1.2	0.97
3 wt.%	30.9 ± 0.8	11.5 ± 1.0	3.6 ± 1.4	0.97

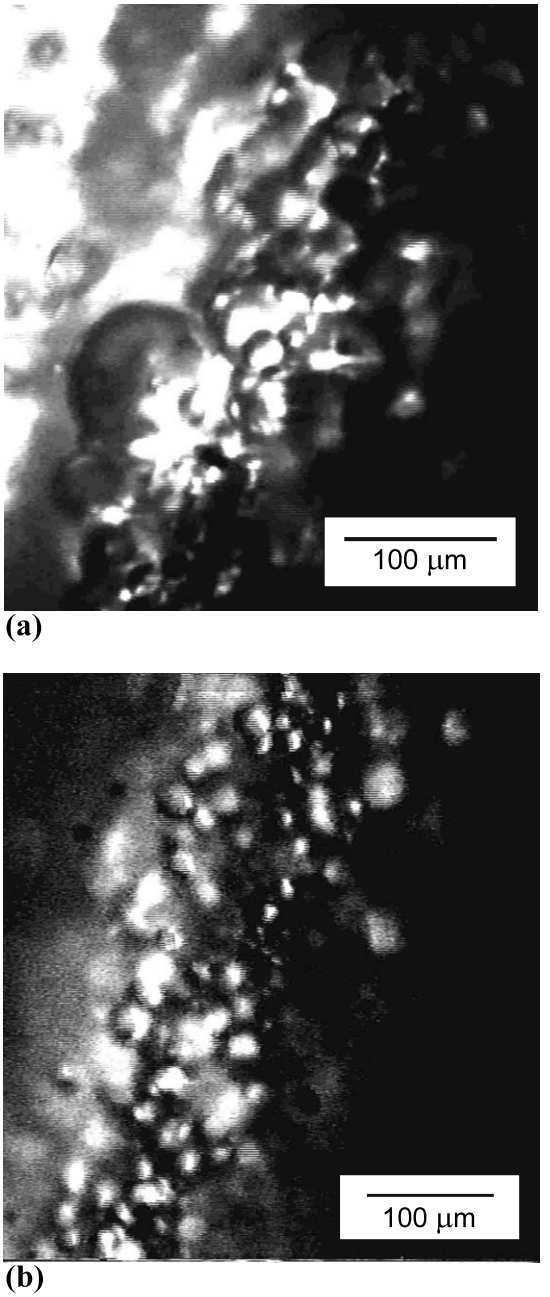

Fig. 7. Photos of the outer surface of a microporous glass membrane taken during the process of emulsification; the drops are of hexadecane in water solutions: (a) 1 wt.% Na-caseinate, pore size 2.1 μm; (b) 1 wt.% BLG, pore size 10.4 μm.

4.3. Dynamic interfacial tension and adsorption rate

One of the reasons for the larger emulsion drops formed in Na-caseinate solutions, in comparison with the BLG solutions (see Fig. 8), can be the difference between the rates of adsorption of these two proteins at the oil–water interface. To check this hypothesis, we carried out measurements of dynamic interfacial tension by means of the fast formed drop (FFD) technique [57,58]. A drop with fresh oil–water interface is produced at

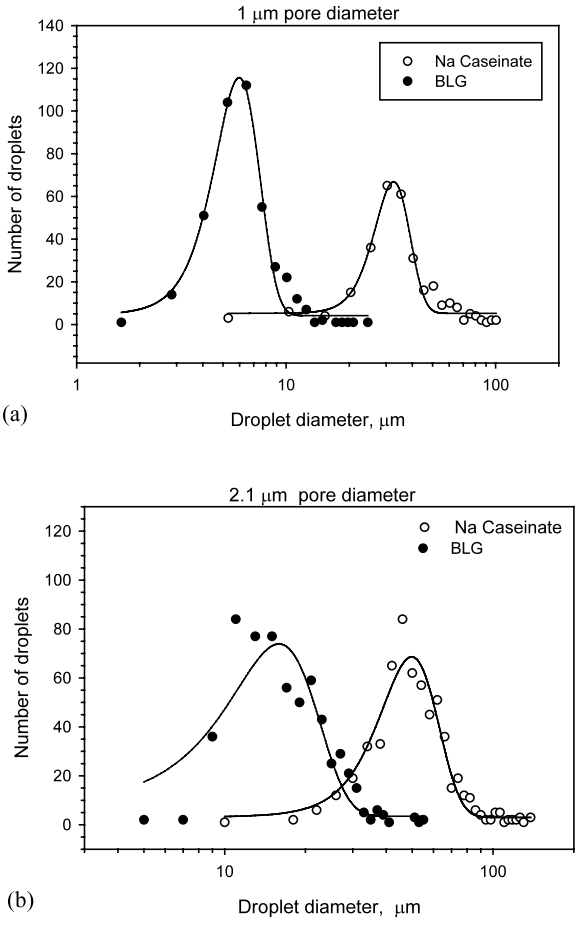

Fig. 8. Size distributions of hexadecane drops produced by membrane emulsification in solutions containing 1 wt.% Na-caseinate or 1 wt.% BLG. (a) Pore diameter 1 μm, size distributions for 413 drops with BLG and for 300 drops with Na-caseinate; (b) pore diameter 2.1 μm, size distribution for 600 drops. The curves are Gaussian fits, see Table 3.

Table 3
Parameters of the Gaussian fits in Figs. 8 and 9 drawn by means of Eq. (1)

Protein concentration	d_m (μm)	b (μm)	N_0	R
Pore diameter 1.0 μm				
1 wt.% BLG	5.8 ± 0.1	1.4 ± 0.1	4.1 ± 2.0	0.98
1 wt.% Na-caseinate	32.9 ± 0.5	6.8 ± 0.5	5.2 ± 1.2	0.97
Pore diameter 2.1 μm				
1 wt.% BLG	15.9 ± 0.7	6.1 ± 0.8	3.5 ± 4.4	0.91
1 wt.% Na-caseinate	50.0 ± 0.7	12.3 ± 0.8	3.0 ± 1.6	0.97
Emulsion obtained by Ultra Turrax				
1 wt.% BLG	2.7 ± 0.1	0.7 ± 0.1	11 ± 5	0.96

the tip of a capillary by a sudden breaking of a jet from the aqueous solution, which flows out of the capillary into the oil phase. The protein (the surfactant) adsorbs at the immobile curved surface of the formed drop, and consequently, the interfacial tension σ, and the pressure inside the drop, decrease with time, t. The pressure is registered by means of a piezo-transducer, whose electric output can be converted in terms of interfacial tension, σ, by using the Laplace equation of capillarity. In this way, the data for the dynamic interfacial tension $\sigma(t)$ in Fig. 10 have been obtained. The capillary pressure has been recorded every 0.005 s, which gives a large number of experimental points and provides a good statistics and time-resolution.

Fig. 10(a) shows the plots of σ versus $t^{1/2}$ during the first 2.5 s of the adsorption process. The data for BLG, at the earlier times, well comply with the dependence

$$\frac{\sigma(t)-\sigma_e}{\sigma(0)-\sigma_e} \approx 1 - 2\left(\frac{t}{\pi t_d}\right)^{1/2} \tag{2}$$

which represents the short-time asymptotics of the interfacial tension in the case of adsorption under diffusion control [50]; σ_e is the solution's equilibrium interfacial tension, while $\sigma(0)$ is the tension of the bare oil–water interface; t_d is the diffusion relaxation time. In contrast, the short time behavior of $\sigma(t)$ for Na-caseinate (Fig. 10(a)) is typical for adsorption under mixed barrier-diffusion control; in such a case, the theoretical dependence $\sigma(t)$ is described by the expression [59]

$$\frac{\sigma(t)-\sigma_e}{\sigma(0)-\sigma_e} = \frac{2}{\pi}\left(\frac{t_d}{t_a}\right)^{1/2} \int_0^\infty \frac{\exp(-t\tau^2/t_a)}{(\tau^2-1)^2 + t_d\tau^2/t_a}\, d\tau \tag{3}$$

where t_a is the adsorption relaxation time which accounts for the existence of a barrier to adsorption. In general, one has [59]

$$t_d = \frac{G^2}{D}, \qquad t_a = \frac{G}{k_a}, \qquad G \equiv \left(\frac{\partial \Gamma}{\partial c}\right)_e \tag{4}$$

D is the diffusivity of the adsorbing surfactant; k_a is the kinetic rate constant of adsorption [59–61]; c and Γ are, respectively, the surfactant concentration and adsorption.

Fig. 10(b) shows the long-time asymptotics of $\sigma(t)$ (for $8 < t < 30$ s) plotted as σ versus $t^{-1/2}$. One sees that the data agree well with the theoretical dependence

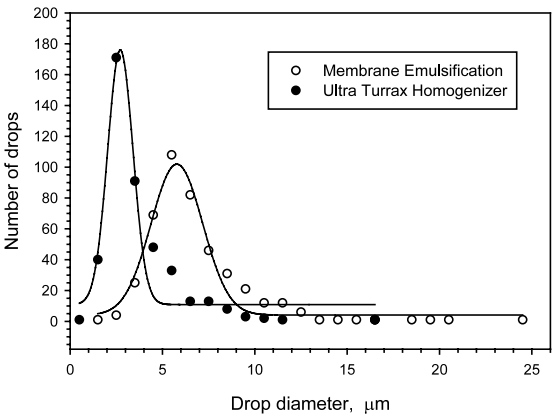

Fig. 9. Comparison of the size distributions of oil drops produced by membrane emulsification (1 μm pore diameter) and by a rotor-stator homogeniser Ultra Turrax in water solutions containing 1 wt.% BLG; the curves are Gaussian fits, see Table 3.

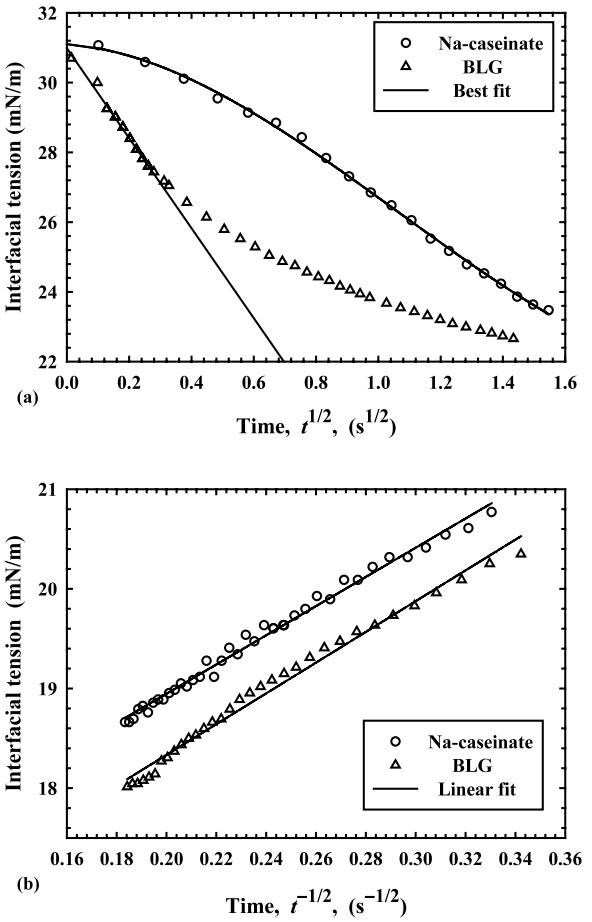

Fig. 10. Comparison between the dynamic interfacial tensions of aqueous solutions of BLG and Na-caseinate against soybean oil: data obtained using the FFD technique [57] at protein concentration 0.02 wt %: (a) short-time asymptotics; (b) long-time asymptotics. The lines are the best theoretical fits, see Table 4.

$$\frac{\sigma(t)-\sigma_e}{\sigma(0)-\sigma_e} \approx \left(\frac{t_d}{\pi t}\right)^{1/2} \quad (5)$$

which corresponds to adsorption under diffusion control. Note that Eqs. (2)–(5) are applicable in two cases: (i) small initial perturbation and (ii) linear (Henry) adsorption isotherm, $\Gamma = Gc$. The latter relationship holds for protein adsorption monolayers at not-too-long adsorption times [62,63]. (At the longer adsorption times, some aging effects are observed with the proteins, which may form an elastic, rather than fluid, interfacial film [64].)

As mentioned above, the data for BLG and Na-caseinate in Fig. 10(a) are fitted, respectively, with Eqs. (2) and (3) The data in Fig. 10(b) are fitted with Eq. (5). The parameter values determined from the best fits are given in Table 4. The values of $\sigma(0)$, obtained from the fits of the data for BLG and Na-caseinate, are coincident with the tension of the bare soybean oil–water interface, $\sigma_0 = 31.1$ mN m^{-1}, as it should be expected. The major difference between the two proteins is the existence of a barrier to adsorption for the Na-caseinate, which is characterized by the adsorption time $t_a = 2.7$ s. The latter is a measure for the average time of stay of the Na-caseinate molecule/aggregate in the subsurface before its adsorption at the surface. The barrier lowers the adsorption rate for Na-caseinate, which, in its own turn, affects the size of the oil drops formed by membrane emulsification (see Section 6 for a more detailed discussion). Indeed, the time of formation of an oil drop at the membrane surface is typically smaller than $t_a = 2.7$ s.

Table 4
Parameters determined from the best fits of the data in Fig. 10

Protein concentration	R	Interfacial tension (mN m^{-1})	t_d (s)	t_a (s)
Short-time asymptotics, Eqs. (2) and (3); Fig. 10(*a*)				
0.02 wt.% BLG	0.995	$\sigma(0) = 31.0 \pm 0.1$	1.9 ± 0.1	–
0.02 wt.% Na-caseinate	0.999	$\sigma(0) = 31.1 \pm 0.1$	1.3 ± 0.2	2.7 ± 0.3
Long-time asymptotics, Eq. (5); Fig. 10(*b*)				
0.02 wt.% BLG	0.993	$\sigma_e = 15.2 \pm 0.1$	3.0 ± 0.1	–
0.02 wt.% Na-caseinate	0.995	$\sigma_e = 16.0 \pm 0.1$	3.0 ± 0.1	–

It is known that in aqueous solutions both BLG and Na-caseinate form polydisperse aggregates, see e.g. [65,66] and the literature cited therein. When the protein diffuses toward a newly created oil-water interface, the smaller aggregates reach the phase boundary earlier, while the larger aggregates arrive later. This is a possible explanation why the characteristic diffusion time, $t_d = G^2/D$, see Table 4, is smaller for the short-time asymptotics and larger for the long-time asymptotics (D is greater for the smaller aggregates which affect the short-time asymptotics, whereas D is smaller for the larger aggregates whose transport influences the long-time asymptotics). Note also, that the values of σ_e in Table 4, determined from the long-time asymptotics (from the intercepts of the lines in Fig. 10(b)), correspond to a fluid protein adsorption layer, before the occurrence of structural changes in this layer.

5. β–Lactoglobulin and Tween 20

We carried out additional experiments in which the aqueous phase was again 1 wt.% BLG with 0.1 g dm^{-3} sodium azide (NaN_3), but we added also a certain amount of the nonionic surfactant Tween 20. It is believed that the molecules of Tween 20 (and of other low-molecular-weight surfactants) adsorb at vacant holes in the interfacial protein network. Thereafter, the surfactant disconnects this network and causes a displacement of the protein molecules [67,68]. The latter are found to form aggregates at the oil–water interface; this action of Tween 20 has been called the 'orogenic effect' [69,70]. Our purpose is to see whether the addition of Tween 20 to the BLG solution would influence the membrane emulsification.

Fig. 11 compares the size distributions of soybean oil drops formed by membrane emulsification (pore diameter 1 μm) in aqueous solutions of 1 wt.% BLG with and without Tween 20. The parameters of the Gaussian fits in Fig. 11 are listed in Table 5. One sees that the addition of Tween 20 slightly decreases the mean drop diameter, 5.1 versus 5.8 μm, but simultaneously it increases the distribution's half-width: 1.8 versus 1.4 μm. We may conclude that the addition of Tween 20 has a weak influence on the emulsions produced by a microporous membrane. We could hypothesize that the reason for the weak effect of Tween 20 is that the drop size is influenced mostly by the adsorption of BLG at the surface of the glass membrane (rather than by the orogenic effects), see Section 6 for details.

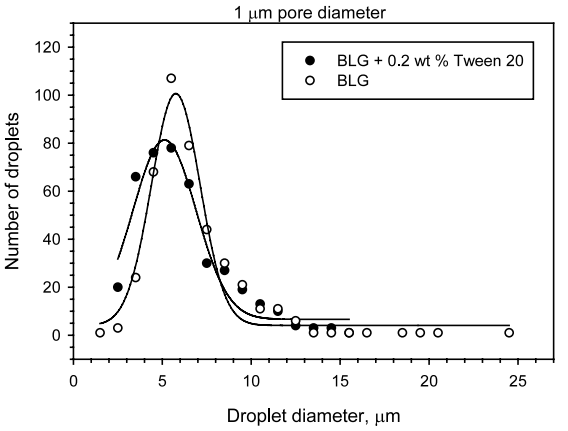

Fig. 11. Comparison of size distributions of soybean oil drops produced by membrane emulsification (pore diameter 1 μm) in solutions containing 1 wt.% BLG without Tween 20 and with 0.2 wt.% Tween 20; for each distribution diameters of 413 drops are measured; the curves are Gaussian fits, see Table 5.

To examine the effect of the type of oil, in Fig. 12 we compare the experimental size distributions of soybean-oil and hexadecane drops, obtained with the same emulsification membrane ($d_{pore} = 2.1$ μm) at transmembrane pressure, $\Delta P = 60$ kPa. The aqueous phase is also the same: 1 wt.% BLG + 0.02 wt.% Tween 20 + 0.1 g l^{-1} NaN_3.

Table 5
Parameters of the Gaussian fits in Figs. 11 and 12 drawn by means of Eq. (1)

System	d_m (μm)	b (μm)	N_0	R
Effect of Tween 20 (Fig. 11; $d_{pore} = 1.0$ μm)				
No Tween 20	5.8 ± 0.1	1.4 ± 0.1	4.1 ± 2.0	0.98
0.2 wt.% Tween 20	5.1 ± 0.1	1.8 ± 0.1	6.6 ± 3.0	0.97
Effect of the type of oil (Fig. 12; $d_{pore} = 2.1$ μm)				
Soybean oil	17.1 ± 0.5	6.5 ± 0.4	2.5 ± 2.1	0.97
Hexadecane	14.7 ± 0.4	4.5 ± 0.4	2.7 ± 2.2	0.97

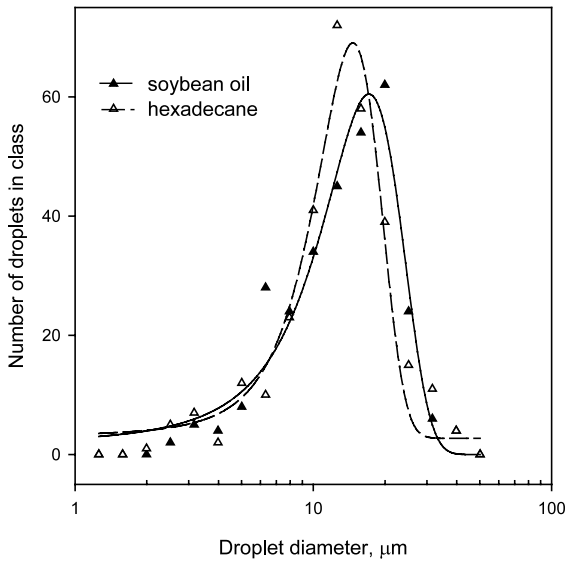

Fig. 12. Comparison of size distributions of soybean oil and hexadecane drops, obtained by membrane emulsification (pore diameter is 2 μm; transmembrane pressure, $\Delta P = 60$ kPa); the aqueous phase is 1 wt.% BLG + 0.02 wt.% Tween 20. For each distribution the diameters of 300 drops are measured; the curves are Gaussian fits, see Table 5.

The viscosities of the two oils differ by more than 17 times: 3 mPa s for hexadecane and above 50 mPa s for the soybean oil. Nevertheless, the difference between the produced emulsions is small (Fig. 12 and Table 5). Still, the more viscous soybean oil produces slightly bigger drops, mean diameter 17.1 versus 14.7 μm, with a slightly broader size distribution, standard deviation 6.5 versus 4.5 μm. The found weak effect of the oil viscosity is consonant with the results by Schröder [21].

6. Discussion and data interpretation

6.1. Two distinct regimes of emulsification

Our direct microscopic observations of the formation and detachment of emulsion drops at the surface of a SPG membrane showed that two regimes of emulsification can be distinguished, depending on the emulsifier type and concentration:

Regime A: almost monodisperse emulsion drops are produced by separate pores. The drops are released quickly, similarly to the bubbles in the case of the known maximum-bubble-pressure method [55,56]. Drops, which stay attached to the membrane surface, are not observed. In this regime, as a rule $d_{drop}/d_{pore} \approx 3$, see e.g. Table 1, and Figs. 2 and 3. Such is the case of O/W emulsions stabilized by Tween 20 (at higher concentrations), by ionic surfactants like sodium dodecyl-sulfate (SDS), and by some egg yolk emulsifiers; similar results have been obtained also with some W/O emulsions; see [2,5,6,14,19,35,36].

Regime B: larger, $d_{drop}/d_{pore} \geq 4$, and relatively polydisperse emulsion drops are formed. The surface of the microporous membrane is covered with a layer of emulsion droplets, which are attached to the membrane, grow with time, and eventually break away. The contact area between an attached drop and the membrane may span several pores at the membrane surface. This regime is observed with Tween 20 at the lower concentrations (Fig. 4(a) and (b) and Fig. 5(a)), as well as for the investigated solutions of Na-caseinate and BLG (see Figs. 6–8 and Tables 3 and 5). $d_{drop}/d_{pore} \geq 4$ has been found for milk proteins and diluted solutions of Tween 20 [8,17,32,34,36].

To get some additional information about the occurrence of the membrane emulsification in regimes A and B, we carried out microscopic observations with a model system: a glass capillary connected to a Hamilton syringe, which supplies the oil phase. A hydrophilic capillary with inner and outer diameters, respectively, 65 and 250 μm, is used. In the beginning of each experiment, the capillary was filled with the aqueous phase (solution of an emulsifier) and, next, the oil phase (hexadecane) was supplied by the syringe. Thus oil drops were released in the water phase one after another. Typical photos are shown in Fig. 13.

For solutions which provide membrane emulsification in Regime A, we observed the presence of water, wetting the inner wall of the capillary in the vicinity of its orifice (Fig. 13(a)). The flux of oil could not remove this water from the capillary

channel. In other words, there is a lasting hydrophilization of the capillary inner wall by the solution of emulsifier. In contrast, for solutions, for which the membrane emulsification occurs in regime B, we did not observe penetration of water inside the capillary, see Fig. 13(b). Although the capillary was initially filled with the aqueous solution, the water phase was completely pushed out by the advancing oil.

We use the photos in Fig. 13 only as an illustration of the effect of hydrophilization of the glass surface around the orifice of a capillary, which probably happens in a similar way for the pore openings of the SPG membranes. On the other hand, the size of the drops released by the microporous membranes and the glass capillary in Fig. 13 is not comparable, because the mechanisms of drop detachment are rather different. In both cases the breaking of the drops occurs through a necking instability, however, in the former case the source of drop deformation is the hydrodynamic flow of oil along the pore, whereas in the latter case the deformation is caused by the buoyancy force due to gravity [51].

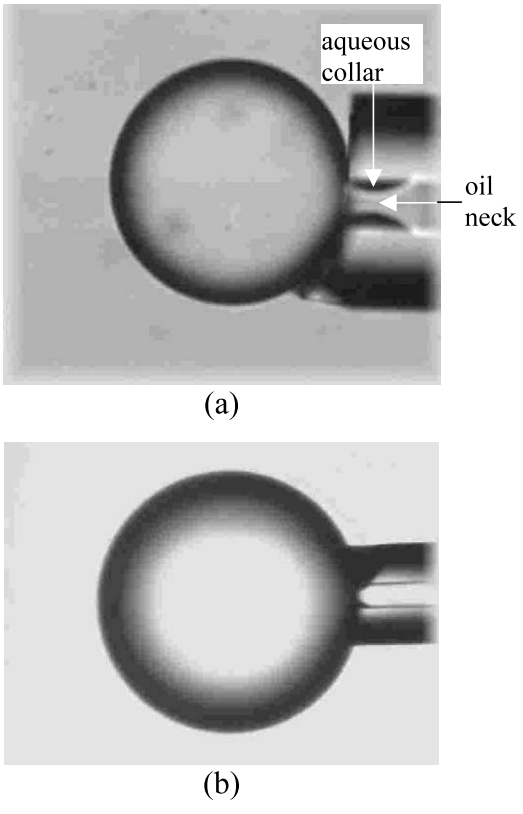

Fig. 13. Photos of a capillary (inner diameter 65 μm) with attached hexadecane droplets; the outer phase is an aqueous solution of (a) 1 wt.% sodium dodecyl benzene sulfonate + 0.012 M NaCl; (b) 1 wt % Na-caseinate.

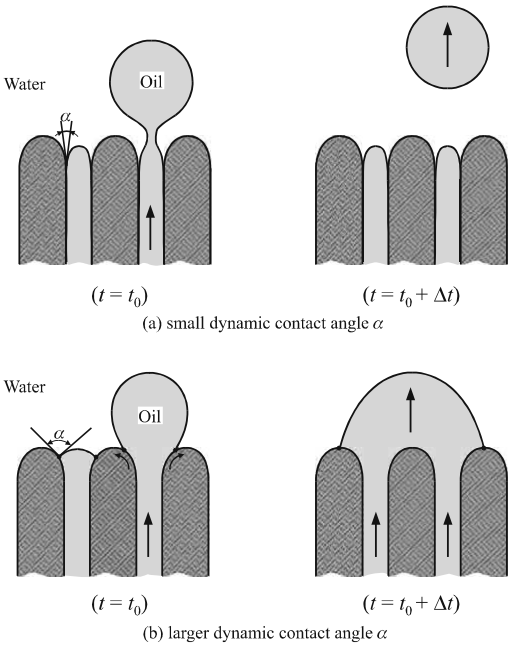

Fig. 14. Sketch of the surface of a microporous membrane at the moment t_0 and in a subsequent moment $t_0 + \Delta t$ during emulsification. (a) The dynamic contact angle α is small and the contact line solid-water-oil is fixed at the pore diameter. (b) The angle α is larger and facilitates the contact-line expansion in the course of growth of the drop; the latter may span two or more pores.

6.2. Role of the dynamic contact angle

First of all, we note again that the formation and detachment of emulsion drops at the surface of a microporous membrane is an essentially dynamic process: its characteristic time is usually ≤ 1 s. Hence, the rate of surfactant adsorption is expected to play an important role. The adsorption rate depends not only on the type of emulsifier, but also on its concentration. For example, the decrease of surfactant concentration leads to an increase of the characteristic adsorp-

tion time by several orders of magnitude; see e.g. [61], Chapter 1.

Fig. 14(a) illustrates the case when the contact angle solid–water–oil, denoted by α, is small, that is the oil does not wet the membrane. In such a case, the expansion of the contact line solid–water–oil is energetically disadvantageous. For that reason, the contact line tends to acquire the smallest possible diameter, which is equal to d_{pore}. In this way, the formation of an oil drop at the orifice of a pore occurs at fixed diameter of the contact line. The drop detachment happens by necking, when the drop volume reaches a critical value; the hydrodynamic theory [51] predicts that in such a case $d_{\text{drop}}/d_{\text{pore}} \approx 3$. In other words, the situation depicted in Fig. 14(a) corresponds to the case, when relatively monodisperse emulsion drops are produced by the microporous membrane, that is to regime A (see above).

Fig. 14(b) illustrates the case of larger contact angle α. In this case, the growth of the drop at the orifice of a pore may cause a disbalance of the forces acting per unit length of the contact line, and the latter will begin to expand. Thus, after the drop pops up from the opening, it does not immediately detach by necking (as in regime A); instead, its contact line expands and the drop spends longer time attached to the membrane. The contact area drop/membrane could span the orifices of two or more pores, and thus, a growing droplet can be fed by several pores (Fig. 14(b)). Moreover, the expansion of the contact line can lead to the appearance of a hydrophobized domain on the membrane surface. Therefore, it turns out that the oil drops can be released by separate hydrophobized domains rather than by the individual pores. Since the hydrophobized domains are greater than the pores, they release larger emulsion drops, as it is in regime B (see above). In addition, since the hydrophobized domains (unlike the individual pores) are polydisperse in size, they would produce polydisperse emulsion drops (see e.g. Fig. 6).

In the first manual on membrane emulsification, Nakashima et al. [2] noted that a fine and monodisperse emulsion can be produced if the membrane is not wetted by the dispersion phase. In other words, one has to ensure small contact angle α, which leads to working regime A. Here, we will discuss in more details the capillary mechanisms influencing the emulsification regimes, and especially, the effect of the dynamic surface tension and the contact-line expansion. The known Young equation, which expresses the force balance per unit length of the solid–water–oil contact line, reads

$$\cos\alpha(t) = \frac{\sigma_{\text{so}} - \sigma_{\text{sw}}}{\sigma_{\text{ow}}(t)} \tag{6}$$

where σ_{so} and σ_{sw} are the superficial tensions of the boundaries solid/oil and solid/water, and $\sigma_{\text{ow}}(t)$ is the interfacial tension of the fluid boundary oil/water. As the latter interface quickly and significantly expands during the emulsification process, then σ_{ow}, and consequently α, will essentially depend on the time of drop formation, t. That is the reason why we term $\alpha(t)$ 'dynamic contact angle'.

Now, having in mind Eq. (6), let us try to explain why the drops formed in the solution of 1 wt.% BLG are considerably smaller than those in 1 wt.% Na-caseinate, see Fig. 8 and Table 3. As mentioned above, for both these solutions the membrane emulsification happens in regime B. In view of the proposed interpretation, the formation of smaller drops in the BLG solutions should correspond to a smaller angle α. Indeed, one can expect that

$$\sigma_{\text{sw}}\,(\text{BLG}) < \sigma_{\text{sw}}\,(\text{Na-caseinate}) \tag{7}$$

$$\sigma_{\text{ow}}\,(\text{BLG}) < \sigma_{\text{ow}}\,(\text{Na-caseinate}) \tag{8}$$

The relationship (Eq. (7)) follows from the experimental fact that BLG (and other globular proteins), unlike Na-caseinate, are found to spontaneously adsorb at the glass–water interface [66], and, consequently, to decrease the surface free energy per unit area, σ_{sw}. In addition, Fig. 10(a) shows that the dynamic interfacial tension $\sigma_{\text{ow}}(t)$ is smaller for BLG in comparison with Na-caseinate, because the latter encounters a kinetic barrier to adsorption at the oil water interface (Section 4.3); for this reason, the relation Eq. (8) holds. Eq. (6) implies that the factors behind Eqs. (7) and (8) act in the same direction, viz. both of them lead to a smaller dynamic contact angle α

for BLG in comparison with Na-caseinate. The latter fact can explain the difference between the two curves in Fig. 8.

Likewise, the dynamic interfacial tension σ_{ow} is expected to be significantly smaller for 2 wt.% Tween 20, in comparison with 0.02 wt. % Tween 20, which could imply $\alpha(2\ \text{wt.\%}) \ll \alpha(0.02\ \text{wt.\%})$, see Eq. (6), and could explain why with the former solution the membrane emulsification happens in regime A, while with the latter solution—in regime B, see Figs. 4 and 5. More precisely, the coexistence of a peak at $d_{drop}/d_{pore} \approx 3$ with considerably larger drops in Fig. 4(a) and (b), indicates that for the lower concentrations of Tween 20 a fraction of the pores remains hydrophilic, while the others are hydrophobized. Hence, one may conclude that in this specific case, we are dealing with a hybrid of regimes A and B.

6.3. Driving force of contact-line expansion

Finally, let us discuss the contact-line expansion (Fig. 14(b)), taking into account the fact that, as a rule, a hysteresis of the contact angle exists on the solid surface, which is not expected to be molecularly smooth. The presence of hysteresis implies that the contact line will begin to expand (the water meniscus will start to recede) when the actual contact angle, α, becomes smaller than a certain critical value, the receding angle α_R; see e.g. [61], Chapter 6. For $\alpha = \alpha_R$ the forces acting per unit length of the contact line are still balanced, that is $\sigma_{ow}\cos\alpha_R + \sigma_{ow} - \sigma_{ow} = 0$. However, for $\alpha < \alpha_R$ the latter balance is violated and the oil begins to spread over the glass. The driving force of oil spreading, Δf, stems from the disbalance of tensions exerted at the contact line, viz.

$$\Delta f = \sigma_{ow}\cos\alpha + \sigma_{sw} - \sigma_{ow} = \sigma_{ow}(\cos\alpha - \cos\alpha_R) \le \sigma_{ow}(1 - \cos\alpha_R) \qquad (9)$$

In regime A (Fig. 14(a)) we have $0 \le \alpha < \alpha_R \ll 1$ and then Eq. (9) predicts that in this regime the driving force Δf will have a vanishingly small value. For example, taking $\alpha_R = 3°$ and $\sigma_{ow} = 10$ mN m^{-1}, from Eq. (9) we estimate $\Delta f \le 0.014$ mN m^{-1}. In other words, in regime A the hypothetical driving force is rather small, and for that reason it is unable to give rise to a contact-line expansion. Indeed, the glass surface is not molecularly smooth and contact line will stick to an edge.

In contrast, in regime B (Fig. 14(b)), the receding angle α_R can be larger, which ensures a greater driving force Δf. The larger Δf prevents the attachment of the contact line to small edges at the glass surface, so spreading of oil on the glass will take place. In particular, to have $\Delta f \ge 1$ mN m^{-1} for $\sigma_{ow} = 10$ mN m^{-1}, a receding contact angle $\alpha_R \ge 26°$ is needed, see Eq. (9). Such, and greater, values of α_R are quite realistic, which explains the reason why the forming emulsion drop is not attached to the opening of the feeding pore in regime B, but instead, the drop spans a wider area of the membrane surface and grows larger in size.

Despite the fact that the above analysis has been done for O/W emulsions, it can be easily adapted to the case of W/O emulsions. In both cases, the general recommendation is the same: To produce a fine and monodisperse emulsion ($d_{drop}/d_{pore} \approx 3$) by means of a microporous membrane, one has to ensure such conditions, that the membrane is not wet by the dispersion phase. In addition, if a cross flow (not considered in the present article) is applied in the continuous phase, one could achieve $d_{drop}/d_{pore} < 3$, see [47].

7. Summary and conclusions

In this paper we investigate the process of membrane emulsification in the presence of the nonionic surfactant Tween 20, and the milk proteins Na-caseinate and BLG. Our goal is to examine the factors which control the drop-size distribution. The emulsion drops are produced at the outer surface of a cylindrical microporous glass membrane (Fig. 1), so that the process of their formation and detachment can be directly observed by optical microscopy.

In the case of 2 wt.% aqueous solution of Tween 20, we obtain relatively monodisperse O/W emulsion with $d_{drop}/d_{pore} \approx 3$, see Fig. 2. The pre-equilibration of the oil and water, with respect to the distribution of Tween 20 between the two phases, has a weak effect on the drop size (Fig. 3

and Table 1). The direct microscopic observations show that monodisperse oil drops intensively pop out of separate pores (Fig. 5(b)). The monodispersity and the small drop size of the produced emulsions can be attributed to the fast kinetics of surfactant adsorption at the oil–water interface which, in accordance with Eq. (6), ensures a good wetting of the membrane surface by the respective surfactant solution under dynamic conditions (Fig. 14(a)).

In contrast, for the lower concentrations of Tween 20, as well as for the investigated solutions of Na-caseinate and BLG, we observe that the membrane is covered by a layer of growing attached emulsion drops, which are polydisperse, with a relatively large mean drop size ($d_{drop}/d_{pore} \geq 5$), see Fig. 4(a) and (b), Fig. 5(a), Figs. 6–8, 11 and 12, and Tables 2, 3 and 5. This fact can be attributed to a greater dynamic contact angle solid-water-oil. In such a case, after a drop protrudes from an opening, it does not immediately detach, but instead, its contact line expands and the contact area drop/membrane could span the orifices of two or more pores. In this way, a growing droplet can be fed by several pores (Fig. 14(b)). The contact-line expansion can lead to the appearance of hydrophobized domains on the membrane surface. Thus, it turns out that the oil drops are released by separate hydrophobized domains rather than by the individual pores. Correspondingly, the size distribution of the formed emulsion drops reflects the size distribution of the hydrophobic domains.

The smaller average size and half-width of the drop distribution in the emulsions stabilized by BLG, in comparison with those stabilized by Na-caseinate (Figs. 7 and 8 and Table 3), can be explained (i) with the spontaneous adsorption of BLG on the membrane surface and (ii) with the fact that BLG has a faster adsorption kinetics at the oil-water interface than the Na-caseinate (the latter encounters a kinetic barrier to adsorption, see Fig. 10 and Table 4). Both these effects lead to diminishing of the dynamic contact angle solid–water–oil, see Eq. (6), and impede the expansion of the drop contact line. In other experiments, we established that the addition of 0.2 wt.% Tween 20 to BLG, and the viscosity of the used oil, have a weak influence on the membrane emulsification, see Figs. 11 and 12.

It is worthwhile nothing that in none of the investigated emulsions (except the case with 0.01 wt.% Na-caseinate) we observed any pronounced coalescence of the oil drops, either on the membrane surface or in the bulk of the produced emulsion. Hence, the generation of larger and polydisperse drops in some of the studied solutions is attributed mostly to the effect of contact-line expansion and formation of hydrophobized domains on the membrane surface. Therefore, any factor which leads to decrease of the dynamic three-phase contact angle α (Fig. 14), and in this way prevents the contact-line expansion, facilitates the production of fine and monodisperse emulsions.

Acknowledgements

This study was supported by the Inco-Copernicus Project, Number IC15CT980911, of the European Commission. The authors are grateful to Mr Luben Arnaudov for the dynamic surface tension measurements and to Professor Ivan B. Ivanov and Dr Theodor Gurkov for the stimulating discussions.

References

[1] T. Nakashima, M. Shimizu, Advanced inorganic separative membranes and their developments, Chem. Eng. Symp. Ser. 21 (1988) 93–99.
[2] T. Nakashima, M. Shimizu, M. Kukizaki (Eds.), Membrane Emulsification Operational Manual, first ed., Department of Chemistry, Industrial Research Institute of Miyazaki Prefecture, Miyazaki, 1991.
[3] K. Kandori, K. Kishi, T. Ishikawa, Formation mechanisms of monodispersed W/O emulsions by SPG filter emulsification method, Colloids Surf. 61 (1991) 269–279.
[4] K. Kandori, K. Kishi, T. Ishikawa, Preparation of uniform silica hydrogel particles by SPG filter emulsification method, Colloids Surf. 62 (1992) 259–262.
[5] T. Nakashima, K. Nakamura, M. Kochi, Y. Iwasaki, M. Tomita, Development of membrane emulsification and its applications to food industries, Nippon Shokuhin Kogyo Gakkaishi 41 (1994) 70–76.

[6] K. Kandori, Applications of microporous glass membranes: membrane emulsification, in: A.G. Gaonkar (Ed.), Food Processing: Recent Developments, Elsevier, Amsterdam, 1995, pp. 113–142.
[7] K. Shiomori, T. Hayashi, T. Hano, Hydrolysis rates of olive oil by lipase in a monodispersed O/W emulsion system using membrane emulsification, J. Ferment. Bioeng. 80 (1995) 552–559.
[8] R. Katoh, Y. Asano, A. Furuya, M. Tomita, Conditions for preparation of O/W food emulsions using a membrane emulsification system, Nippon Shokuhin Kagaku Kogaki Kaishi 42 (1995) 548–555.
[9] R. Katoh, Y. Asano, A. Furuya, K. Sotoyama, M. Tomita, Preparation of food emulsions using a membrane emulsification system, J. Membrane Sci. 113 (1996) 131–135.
[10] K. Suzuki, I. Shuto, Y. Hagura, Characteristics of the membrane emulsification method combined with preliminary emulsification for preparing corn oil-in-water emulsions, Food Sci. Technol. Int. 2 (1996) 43–47.
[11] S. Omi, K. Katami, T. Taguchi, K. Kaneko, M. Iso, Synthesis and applications of porous SPG (Shirasu Porous Glass) microspheres, Macromol. Symp. 92 (1995) 309–320.
[12] H. Yoshizawa, H. Ohta, Y. Hatate, Novel procedure for monodispersed polymeric microspheres with high electrifying additive content by particle-shrinking method via SPG membrane emulsification, J. Chem. Eng. Jpn. 29 (1996) 1027–1029.
[13] S. Higashi, M. Shimizu, T. Nakashima, K. Iwata, F. Uchiyama, S. Tateno, S. Tamura, T. Setoguchi, Arterial-injection chemotherapy for hepatocellular carcinoma using monodisperse poppy-seed oil microdroplets containing fine aqueous vesicles of epirubicin: initial medical application of a membrane-emulsification technique, Cancer 75 (1995) 1245–1254.
[14] Y. Mine, M. Shimizu, T. Nakashima, Preparation and stabilization of simple and multiple emulsions using a microporous glass membrane, Colloids Surf. B 6 (1996) 261–268.
[15] H. Kage, H. Kawahara, H. Ogura, Y. Matsuno, Complex coacervation microencapsulation of mono-dispersed droplets prepared by membrane emulsification, Kagaku Kogaku Ronbunshu 23 (1997) 652–658.
[16] H. Okochi, M. Nakano, Comparative study of two preparation methods of W/O/W emulsions: stirring and membrane emulsification, Chem. Pharmaceut. Bull. 45 (1997) 1323–1328.
[17] R. Katoh, Y. Asano, A. Furuya, K. Sotoyama, M. Tomita, S. Okonogi, Methods for preparation of W/O food emulsions using the membrane immersed with oils and fats, Nippon Shokuhin Kagaku Kogaki Kaishi 44 (1997) 238–242.
[18] Y. Hatate, H. Ohta, Y. Uemura, K. Ijichi, H. Yoshizawa, Preparation of monodispersed polymeric microspheres for toner particles by the Shirasu porous glass membrane emulsification technique, J. Appl. Polym. Sci. 64 (1997) 1107–1113.
[19] V. Schröder, O. Behrend, H. Schubert, Effect of dynamic interfacial tension on the emulsification process using microporous, ceramic membranes, J. Colloid Interface Sci. 202 (1998) 334–340.
[20] V. Schröder, H. Schubert, Production of emulsions using microporous, ceramic membranes, Colloids Surf. A 152 (1999) 103–109.
[21] V. Schröder, Herstellen von Öl-in-Wasser-Emulsionen mit mikroporösen Membranen, Ph.D. Thesis, University of Karlsruhe, Shaker Verlag, Aachen, 1999.
[22] S.J. Peng, R.A. Williams, Controlled production of emulsions using a crossflow membrane, Part. Part. Syst. Charact. 15 (1998) 21–25.
[23] S.J. Peng, R.A. Williams, Controlled production of emulsions using a crossflow membrane. Part I: Droplet formation from a single pore, Trans. IchemE 76 (1998) 894–901.
[24] R.A. Williams, S.J. Peng, D.A. Wheeler, N.C. Morley, D. Taylor, M. Whalley, D.W. Houldsworth, Controlled production of emulsions using a crossflow membrane. Part II: Industrial scale manufacture, Trans. IchemE 76 (1998) 902–910.
[25] Y.-K. Ha, H.J. Lee, J.H. Kim, Large and monodispersed polymeric microspheres with high butadiene content via membrane emulsification, Colloids Surf. A 145 (1998) 281–284.
[26] S. Nagashima, S. Ando, T. Tsukamoto, H. Ohshima, K. Makino, Preparation of monodisperse poly(acrylamide-co-acrylic acid) hydrogel microspheres by a membrane emulsification technique and their size-dependent surface properties, Colloids Surf. B 11 (1998) 47–56.
[27] S. Nagashima, M. Koide, S. Ando, K. Makino, T. Tsukamoto, H. Ohshima, Surface properties of monodisperse poly(acrylamide-co-acrylic acid) hydrogel microspheres prepared by a membrane emulsification technique, Colloids Surf. A 153 (1999) 221–227.
[28] Y.K. Ha, H.S. Song, H.J. Lee, J.H. Kim, Preparation of core particles for toner application by membrane emulsification, Colloids Surf. A 162 (1999) 289–293.
[29] G.H. Ma, M. Nagai, S. Omi, Study on preparation and morphology of uniform artificial polystyrene-poly(methyl methacrylate) composite microspheres by employing the SPG (Shirasu Porous Glass) membrane emulsification technique, J. Colloid Interface Sci. 214 (1999) 264–282.
[30] G.H. Ma, M. Nagai, S. Omi, Effect of lauryl alcohol on morphology of uniform polystyrene-poly(methyl methacrylate) composite microspheres prepared by porous glass membrane emulsification technique, J. Colloid Interface Sci. 219 (1999) 110–128.
[31] G.H. Ma, M. Nagai, S. Omi, Preparation of uniform poly(lactide) microspheres by employing the Shirasu Porous Glass (SPG) emulsification technique, Colloids Surf. A 153 (1999) 383–394.
[32] I. Scherze, K. Marzilger, G. Muschiolik, Emulsification using micro porous glass (MPG): surface behavior of milk proteins, Colloids Surf. B 12 (1999) 213–221.
[33] Y. Asano, K. Sotoyama, Viscosity change in oil/water food emulsions prepared using a membrane emulsification system, Food Chem. 66 (1999) 327–331.

[34] K. Sotoyama, Y. Asano, K. Ihara, K. Takahashi, K. Doi, Water/oil emulsions prepared by the membrane emulsification method and their stability, J. Food Sci. 64 (1999) 211–215.
[35] S.M. Joscelyne, G. Trägårdh, Food emulsions using membrane emulsification: conditions for producing small droplets, J. Food Eng. 39 (1999) 59–64.
[36] S.M. Joscelyne, G. Trägårdh, Membrane emulsification—a literature review, J. Membrane Sci. 169 (2000) 107–117.
[37] H. Yuyama, T. Watanabe, G.H. Ma, M. Nagai, S. Omi, Preparation and analysis of uniform emulsion droplets using SPG membrane emulsification technique, Colloids Surf. A 168 (2000) 159–174.
[38] H. Yuyama, K. Yamamoto, K. Shirafuji, M. Nagai, G.H. Ma, S. Omi, Preparation of polyurethane-urea (PUU) uniform spheres by SPG membrane emulsification technique, J. Appl. Polym. Sci. 77 (2000) 2237–2245.
[39] H. Yuyama, T. Hashimoto, G.H. Ma, M. Nagai, S. Omi, Mechanism of suspension polymerization of uniform monomer droplets prepared by glass membrane (Shirasu Porous Glass) emulsification technique, J. Appl. Polym. Sci. 78 (2000) 1025–1043.
[40] T. Kawakatsu, Y. Kikuchi, M. Nakajima, Regular-sized cell creation in microchannel emulsification by visual microprocessing method, J. Am. Oil Chemists Soc. 74 (1997) 317–321.
[41] T. Kawakatsu, H. Komori, M. Nakajima, Y. Kikuchi, T. Yonemoto, Production of monodispersed oil-in-water emulsion using crossflow-type silicon microchannel plate, J. Chem. Eng. Jpn. 32 (1999) 241–244.
[42] J. Tong, M. Nakajima, H. Nabetani, Y. Kikuchi, Surfactant effect on production of monodispersed microspheres by microchannel emulsification method, J. Surfactants Detergents 3 (2000) 285–293.
[43] T. Kawakatsu, G. Trägårdh, Y. Kikuchi, M. Nakajima, H. Komori, T. Yonemoto, Effect of microchannel structure on droplet size during crossflow, J. Surfactants Detergents 3 (2000) 295–302.
[44] S. Sugiura, M. Nakajima, M. Seki, Preparation of monodispersed solid lipid microspheres using a microchannel emulsification technique, J. Colloid Interface Sci. 227 (2000) 95–103.
[45] P.B. Umbanhowar, V. Prasad, D.A. Weitz, Monodisperse emulsion generation via drop break off in a coflowing stream, Langmuir 16 (2000) 347–351.
[46] P.M. Heertjes, L.H. de Nie, H.J. de Vries, Drop formation in liquid-liquid systems. I. Prediction of drop volumes at moderate speed of formation, Chem. Eng. Sci. 26 (1971) 441–449.
[47] R. Ito, Y. Hirata, K. Inoue, Y. Kitagawa, Formation of a liquid drop at a single nozzle in a uniform stream, Int. Chem. Eng. 20 (1980) 616–620.
[48] Y. Kawase, J.J. Ulbrecht, Formation of drops and bubbles in flowing liquids, Ind. Eng. Chem. Process Des. Dev. 20 (1981) 636–640.
[49] M.A. Hubbe, Theory of detachment of colloidal particles from flat surfaces exposed to flow, Colloids Surf. 12 (1984) 151–178.
[50] P. Joos, Dynamic Surface Tension, VSP BV, Amsterdam, 1999.
[51] K.D. Danov et al., J. Colloid Interface Sci., manuscript in preparation.
[52] K.D. Danov, P.A. Kralchevsky, I.B. Ivanov, Dynamic processes in surfactant stabilized emulsions, in: J. Sjöblom (Ed.), Encyclopedic Handbook of Emulsion Technology, Marcel Dekker, New York, 2001, pp. 621–659 Chapter 26.
[53] O.D. Velev, T.D. Gurkov, R.P. Borwankar, Spontaneous cyclic dimpling in emulsion films due to surfactant mass transfer between the phases, J. Colloid Interface Sci. 159 (1993) 497–501.
[54] O.D. Velev, T.D. Gurkov, I.B. Ivanov, R.P. Borwankar, Abnormal thickness and stability of nonequilibrium liquid films, Phys. Rev. Lett. 75 (1995) 264–267.
[55] T.S. Horozov, C.D. Dushkin, K.D. Danov, L.N. Arnaudov, O.D. Velev, A. Mehreteab, G. Broze, Effect of the surface expansion and wettability of the capillary on the dynamic surface tension measured by the maximum bubble pressure method, Colloids Surf. A 113 (1996) 117–126.
[56] N.A. Mishchuk, S.S. Dukhin, V.B. Fainerman, V.I. Kovalchuk, R. Miller, Hydrodynamic processes in dynamic bubble pressure experiments. Part 5. The adsorption at the surface of a growing bubble, Colloids Surf. A 192 (2001) 157–175.
[57] T. Horozov, L. Arnaudov, A novel fast technique for measuring dynamic surface and interfacial tension of surfactant solutions at constant interfacial area, J. Colloid Interface Sci. 219 (1999) 99–109.
[58] T. Horozov, L. Arnaudov, Adsorption kinetics of some polyethylene glycol octylphenyl ethers studied by the fast formed drop technique, J. Colloid Interface Sci. 222 (2000) 146–155.
[59] K.D. Danov, D.S. Valkovska, P.A. Kralchevsky, Adsorption relaxation for nonionic surfactants under mixed barrier-diffusion and micellization-diffusion control, J. Colloid Interface Sci. (2002) in press.
[60] J.F. Baret, Theoretical model for an interface allowing a kinetic study of adsorption, J. Colloid Interface Sci. 30 (1969) 1–12.
[61] P.A. Kralchevsky, K. Nagayama, Particles at Fluid Interfaces and Membranes, Elsevier, Amsterdam, 2001.
[62] D.E. Graham, M.C. Phillips, Proteins at liquid interfaces: II. Adsorption isotherms, J. Colloid Interface Sci. 70 (1979) 415–426.
[63] T. Sengupta, L. Razumovsky, S. Damodaran, Energetics of protein–interface interactions and its effect on protein adsorption, Langmuir 15 (1999) 6991–7001.
[64] J.T. Petkov, T.D. Gurkov, B.E. Campbell, R.P. Borwankar, Dilatational and shear elasticity of gel-like protein layers on air/water interface, Langmuir 16 (2000) 3703–3711.

[65] K. Koczo, A.D. Nikolov, D.T. Wasan, R.P. Borwankar, A. Gonsalves, Layering of sodium caseinate submicelles in thin liquid films–a new stability mechanism in food dispersions, J. Colloid Interface Sci. 178 (1996) 694–702.
[66] T.D. Dimitrova, F. Leal-Calderon, T.D. Gurkov, B. Campbell, Disjoining pressure vs. thickness isotherms of thin emulsion films stabilized by proteins, Langmuir 17 (2001) 8069–8077.
[67] E. Dickinson, S.R. Euston, C.M. Woskett, Competitive adsorption of food macromolecules and surfactants at the oil–water interface, Prog. Colloid Polym. Sci. 82 (1990) 65–75.
[68] C.M. Wijmans, E. Dickinson, Brownian dynamics simulation of the displacement of a protein monolayer by competitive adsorption, Langmuir 15 (1999) 8344–8348.
[69] A.R. Mackie, A.P. Gunning, P.J. Wilde, V.J. Morris, Orogenic displacement of protein from the oil/water interface, Langmuir 16 (2000) 2242–2247.
[70] A.R. Mackie, A.P. Gunning, M.J. Ridout, P.J. Wilde, V.J. Morris, Orogenic displacement in mixed β-lactoglobulin/β-casein films at the air/water interface, Langmuir 17 (2001) 6593–6598.